Neutron Diffraction from the Vortex Lattice in the Heavy-Fermion Superconductor UPt_3

R. N. Kleiman,[a] C. Broholm,[b] G. Aeppli, E. Bucher,[c] N. Stücheli,[d] and D. J. Bishop
AT&T Bell Laboratories, Murray Hill, New Jersey 07974

K. N. Clausen, K. Mortensen, J. S. Pedersen, and B. Howard[e]
Risø National Laboratory, Roskilde, Denmark
(Received 8 June 1992)

We have used neutron diffraction to observe the vortex lattice of UPt_3. This is the first such measurement in a heavy-fermion system, a superconductor below 1 K, or in a system with such a long magnetic penetration depth (6000 ± 75 Å). It also provides the first value for the pair coherence length, 111 ± 2 Å, to be obtained directly within the pairing state of UPt_3. The lattice is oblique hexagonal with conventional quantization. Its anisotropy can be explained by considering a combination of gap and Fermi-surface anisotropies. The lattice does not appear to change near the transitions between the superconducting phases identified by other techniques.

PACS numbers: 74.70.Tx, 61.12.Bt, 74.60.Ge

There is considerable indirect evidence that the heavy-fermion material UPt_3 is not a conventional s-wave superconductor [1]. This evidence consists primarily of the observation of power-law, rather than exponential, behavior in its thermal and transport properties. Transverse ultrasound [2] and muon spin relaxation (μ^+SR) measurements [3] show different power laws for different crystalline directions in a manner consistent with the E_{1g} symmetry [4]. Further indications of higher-l pairing lie in torsional oscillator [5], ultrasound [6], and specific-heat measurements [7] which show evidence for possible phase transitions within the superconducting state. At $T=0$ ultrasound anomalies occur [8] when $H \approx 0.65 H_{c2}$ ($\mathbf{H} \| \hat{\mathbf{c}}$) and $H \approx 0.25 H_{c2}$ ($\mathbf{H} \perp \hat{\mathbf{c}}$). Since the transition occurs as a function of magnetic field, i.e., vortex density, and the probes observing it are sensitive to vortex motion, it is natural to suggest [9] that this transition corresponds to changes in the vortex lattice at this field. Because of this and the possibility that the unconventional superconducting state manifests itself directly in the vortex lattice, we have used neutron diffraction to study the vortex lattice in UPt_3.

Our sample is a right circular cylinder ≈ 5 mm in diameter and 30 mm long oriented with $\hat{\mathbf{c}}$ along the cylinder axis. The boule was Czochralski grown and float zone purified, and then annealed in vacuum for 150 h at 1300 °C and cooled slowly to room temperature. The extrapolated $T=0$ resistivity along the $\hat{\mathbf{a}}$ axis was 1.3 $\mu\Omega$ cm, equivalent to a mean free path $l \sim 1700$ Å, and the superconducting transition in zero field was clearly split (from specific-heat measurement [10]), with $T_c^- = 0.451$ and $T_c^+ = 0.507$ K.

Neutron scattering from the vortex lattice was first suggested by de Gennes and Matricon [11], first measured in niobium by Cribier *et al.* [12], and subsequently observed in a number of cubic materials [13–15], in technetium [15], and in $YBa_2Cu_3O_7$ [16]. Our experiment was performed using the small-angle neutron scattering (SANS) apparatus in the cold-neutron guide hall of the Risø DR3 reactor. A 6-m-pinhole collimator gave incident beam divergences of $\sim 0.14°$ FWHM (horizontal) and $\sim 0.30°$ FWHM (vertical). The dimensions of the beam impinging on the sample were 4.5 mm (horizontal) $\times 25$ mm (vertical). The incident neutron wavelength λ_n was varied between 5.4 and 13 Å, and the bandwidth $\Delta\lambda/\lambda$ fixed at 18% or 36% by a mechanical velocity selector. The diffracted neutrons were counted by an area detector at the end of a 6-m evacuated chamber. The sample was mounted on the mixing chamber of a dilution refrigerator with the beam along the crystal $\hat{\mathbf{a}}$ axis and with the $\hat{\mathbf{c}}$ axis vertical. A horizontal magnetic field applied along the beam direction was produced by a superconducting magnet operated in persistent mode and fixed relative to the sample. The data discussed here were taken at $T \sim 50$ mK, in applied fields $1.25 < H < 10$ kG arrived at by field cooling the sample from above T_c. There is a substantial small-angle scattering background, primarily from the aluminum cryostat windows; thus all data presented are the differences between raw data and backgrounds collected at 50 mK and $H=0$ or at fixed field and $T > T_c$. A modest correction to the reflectivities was required due to the measured wavelength dependence of the sample transmission.

Our principal result, shown in Fig. 1, is a two-dimensional intensity profile representing the diffraction pattern in the ($\hat{\mathbf{a}}^*$,$\hat{\mathbf{c}}^*$) plane from the vortex lattice at $H=4.25$ kG. There are six clearly observable Bragg peaks forming a distorted hexagonal lattice. The vortex lattice was in all cases a single crystal; thus it was necessary to rotate the cryostat about axes normal to the beam direction to fulfill the Bragg conditions. The data were taken by counting at a number of angles, in increments chosen to fully subtend the rocking curves, thus sweeping out a three-dimensional volume of reciprocal space. The background is radially symmetric and can be expressed as $I_{\rm bkg} = 3.5 \times 10^{-5}/\tau^3$, where τ is in units of Å^{-1} and $I_{\rm bkg}$ is in the same units as shown in Fig. 1.

The rocking curve is quite narrow with $\Delta\theta \sim 0.40°$ FWHM, but considerably broader than expected from purely instrumental broadening ($\Delta\theta \sim 0.15°$ FWHM).

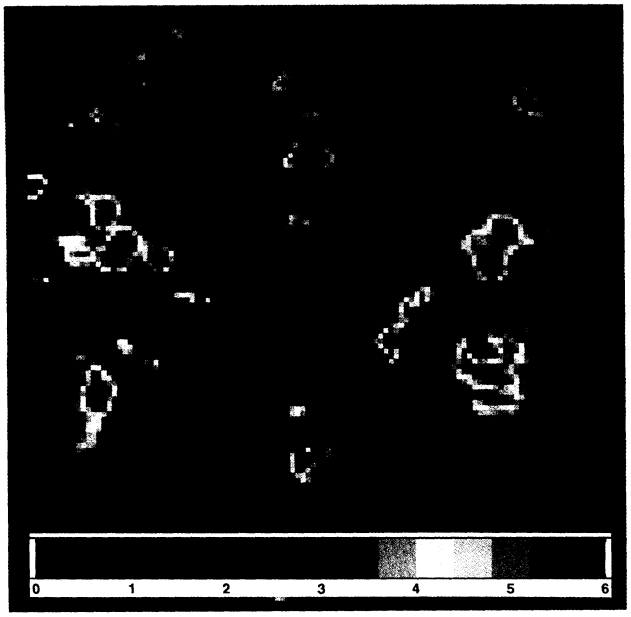

FIG. 1. The 2D intensity profile of the $(\hat{\mathbf{a}}^*,\hat{\mathbf{c}}^*)$ plane of the vortex lattice in UPt_3. The $\hat{\mathbf{c}}^*$ axis is vertical, and the $\hat{\mathbf{a}}^*$ axis is horizontal. The region shown (± 0.0159 Å^{-1}, ± 0.0158 Å^{-1}) corresponds to 60×60 pixels. The intensities are in units of counts/h pixel. The data were taken at $H=4.25$ kG, $T=50$ mK, with $\lambda_n=9.78$ Å and $\Delta\lambda/\lambda=0.36$, using $H=4.25$ kG, $T=600$ mK as a background and represent a total counting time of ≈ 33 h. The integrated intensity of one of the Bragg peaks corresponds to ≈ 250 counts/h. The statistical errors in the peak intensities are $\approx 10\%$. The background scattering is discussed quantitatively in the text.

This implies a mosaic of 0.37°, of which 0.20° can be accounted for by the mosaic of the crystal, and the remaining 0.30° is likely due to the inhomogeneity of the magnetic field over the sample volume. For this diffraction geometry, the order along the flux lines is measured by the rocking curve width, and we find that the vortices are straight over a 3-μm length scale. The shape and orientation of the Bragg peaks in Fig. 1 are, however, correctly accounted for by resolution effects, implying that the correlation lengths for the vortex lattice are in excess of 2000 and 1000 Å parallel to the $\hat{\mathbf{a}}^*$ and $\hat{\mathbf{c}}^*$ directions, respectively.

The vortex lattice in Fig. 1 is quite distorted from the usual hexagonal lattice. This is a consequence of the anisotropy of the underlying lattice and electronic system, since the vortex currents circulate in the $(\hat{\mathbf{a}}^*,\hat{\mathbf{c}}^*)$ plane. A number of authors [17–19] have shown in the anisotropic London (AL) theory, by minimizing the free energy with respect to distortion angle, that for $\mathbf{H}\perp\hat{\mathbf{c}}$, a simple closed form expression results, $\tan^2\alpha=m_3/3m_1$, for the type (b) lattice (see Ref. [20] for notation). Here α is the angle between the $\hat{\mathbf{a}}^*$ axis and the first Bragg peak, and m_1 and m_3 are the reduced effective masses describing the currents $\perp\hat{\mathbf{c}}$ and $\|\hat{\mathbf{c}}$, respectively, normalized so that $m_1^2m_3=1$.

From Fig. 1 we find $\alpha=20.9\pm 0.5°$, giving $m_1/m_3=2.3\pm 0.1$. This can be compared to measurements of this quantity in the normal and superconducting state. Resistivity measurements [21] give $m_1/m_3\sim 1.50$ by assuming that the T^2 coefficient at low temperatures is proportional to $(m^*/m)^2$. Band structure calculations [22] and de Haas–van Alphen measurements [23] provide a detailed understanding of the Fermi surface, but the ratio m_1/m_3 has not yet been calculated, to our knowledge. Penetration depth measurements by μ^+SR give [3] $m_1/m_3=1.1$. $H_{c2}(0)$ values [24,25] give $m_1/m_3=0.65$, whereas $H'_{c2}(1)$ values [24,25] give $m_1/m_3=1.89$ (see Ref. [26] for notation).

In the AL theory the mass tensor is given in a purely phenomenological way, but we wish to understand its microscopic origin. There is a prescription [27] for calculating the mass tensor, given the gap function and the Fermi surface:

$$\frac{1}{m_{ij}}=\frac{\frac{3}{2}\int v_iv_j\delta^2(\hat{\mathbf{k}})d\sigma_F/v_F}{\varepsilon_F\int d\sigma_F/v_F}, \tag{1}$$

where v_F and ε_F are the Fermi velocity and energy, the v_i are components of the Fermi velocity, $\delta(\hat{\mathbf{k}})$ is the momentum-dependent part of the gap function, and $d\sigma_F$ is an element of area of the Fermi surface. In considering the consequences of an anisotropic gap function it has become common to make the *ad hoc* assumption of a spherical Fermi surface, and a particular gap function. Clearly this is not correct since uniaxial anisotropy is allowed in a hexagonal crystal, and its omission forces the interpretation of the normal-state anisotropies as gap anisotropies. To the extent that the normal-state anisotropy is known, our measurement of the superconducting-state anisotropy can be used to determine the anisotropy of the gap state at $T=0$. Note that this determination makes no assumptions about the excitation spectrum. We briefly discuss the case of the E_{1g} state and an ellipsoidal Fermi surface. For this state, $\delta^2(\hat{\mathbf{k}})=\sin^2(\theta)\cos^2(\theta)$ which gives $(m_1/m_3)_S=1.5(m_1/m_3)_N$, where $(m_1/m_3)_N$ is the usual effective mass anisotropy arising from the Fermi surface. If we assume a spherical Fermi surface, this gives $(m_1/m_3)_S=1.5$ in poor agreement with our observed result. However, using the resistivity measurements to estimate $(m_1/m_3)_N\sim 1.50$ gives $(m_1/m_3)_S\sim 2.25$ in reasonable agreement with our experimental observation.

We have performed the same measurement as in Fig. 1 at other fields in the range $1.25<H<10$ kG. The results of the field dependence are summarized in Fig. 2. In Fig. 2(a) we plot the effective field, $B=\phi_0A_K/4\pi$, we measure (based on single flux quantization) versus the applied field, H. Since it is known [3] that $H_{c1}\leq 13$ G, no substantial correction for the sample magnetization is required. We see no evidence at any field for a significant deviation from the expected quantization. Therefore we fix $B=H$ for the remaining analysis, to minimize the errors in the other quantities of interest.

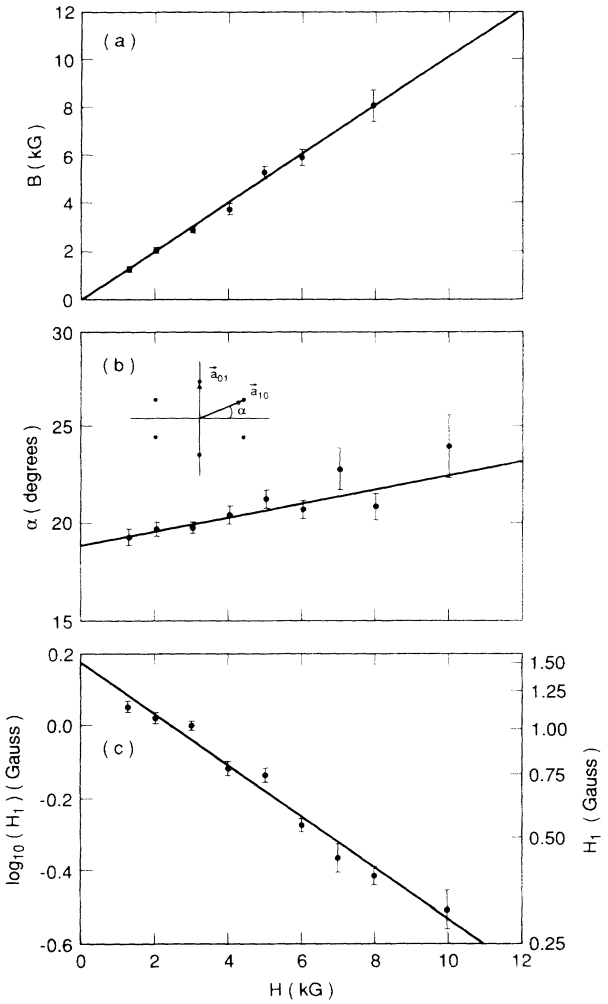

FIG. 2. Extracted parameters from a series of data as in Fig. 1, taken for $1.25 < H < 10$ kG at $T = 50$ mK, with 5.4 Å $< \lambda_n < 13$ Å, and $\Delta\lambda/\lambda = 0.18$. (a) The apparent field B as derived from the unit cell size plotted vs H. [Two points have been omitted from (a) because the fits were unstable.] For (b) and (c) we have fixed $B = H$. (b) The opening angle α plotted vs H. The Bragg peak notation is shown in the inset. The value $\alpha = 20.9°$ gives $m_1/m_3 \simeq 2.28$. (c) The first Fourier coefficient H_{10} plotted on a logarithmic scale vs H. The slope of the line through the data determines ξ, and the intercept determines λ, using Eqs. (2) and (3) from the text.

Figure 2(b) shows the opening angle α versus applied field. In a conventional isotropic superconductor the lattice is triangular ($\alpha = 30°$) and α is independent of the applied field. However, there is a tendency in the data for α to increase with increasing field. The data are described by a linearly increasing function, $\alpha = \alpha_0 + \alpha' H$, where $\alpha_0 = 18.8 \pm 0.3°$ and $\alpha' = 0.37 \pm 0.07°$/kG.

From the AL theory, the form factors for the vortex-lattice Bragg peaks can be calculated [17]. When $\mathbf{H} \perp \hat{\mathbf{c}}$, the form factors for the six primary Bragg peaks in the low-field London limit are $H_{10} = H_{01} = H_1$, with $H_1 = B/[1 + (m_1 m_3)^{1/2} \lambda^2 k_0^2]$, where we have defined $k_0^2 = 8\pi^2 B/\sqrt{3}\phi_0$. At the intermediate fields relevant for our measurement, the vortex core size is significant as compared to the vortex lattice constant, i.e., the smearing of the field distribution due to the nonzero core size must be accounted for. The leading correction to the London theory is given [28] within the Ginzburg-Landau (GL) theory by multiplying the form factors by $\exp[-\xi^2 k_0^2/2(m_1 m_3)^{1/2}]$. Using the fact that $\lambda k_0 \gg 1$ we obtain

$$H_1 = \frac{\phi_0}{\lambda^2} \frac{\sqrt{3}}{8\pi^2} \frac{1}{(m_1 m_3)^{1/2}} e^{-4\pi^2 B \xi^2/\phi_0 (3 m_1 m_3)^{1/2}}, \qquad (2)$$

where λ and ξ have their usual meanings for an anisotropic system.

Figure 2(c) shows that to a very good approximation, $\log_{10}(H_{10})$ decreases linearly with applied field. From the slope of Fig. 2(c) we can determine that $\xi_\perp \sim 121 \pm 2$ Å. (The subscripts on λ and ξ denote the field direction relative to the $\hat{\mathbf{c}}$ direction. The principal values are given in conventional notation.) Using the effective mass anisotropies obtained from α we can deduce the value for the other field orientation. We find that $\xi_\parallel = 93 \pm 3$ Å. These can also be expressed as $\xi_1 = \xi_\parallel$ and $\xi_3 = 157 \pm 4$ Å. Using $\xi_{ave}^3 = \xi_1^2 \xi_3 = \xi_\perp^2 \xi_\parallel$ we get $\xi_{ave} = 111 \pm 2$ Å. While the upper critical fields are not easily amenable to a straightforward GL analysis (see Ref. [26]) we define $H_{c2} = (H_{c2\parallel} H_{c2\perp}^2)^{1/3} = \phi_0/2\pi\xi_{c2}^2$ which gives $\xi_{c2} \sim 119$ Å in quite reasonable agreement with the above value. Also our result for ξ is consistent with our observation [3] that the μ^+SR relaxation rate is greatly reduced in increasing magnetic fields.

Because λ is very long in this system it was not possible to measure it by probing the crossover of $1 + \lambda^2 k^2$. Nevertheless, by measuring the absolute integrated reflectivities, given [29] by

$$R_1 = \frac{\gamma^2 \lambda_n^3 t}{32 \phi_0^2 \sin\theta} H_1^2, \qquad (3)$$

where $\gamma = \mu_n/\mu_N = 1.91$ and t is the average sample thickness in the beam, the H_1 values can be determined in absolute units. From Eq. (2) we see that $\lambda_\perp$ can then be determined from the intercept of the line in Fig. 2(c) at $H = 0$ and we find $\lambda_\perp = 5490 \pm 70$ Å. Combining this with the mass ratios given by α we find that $\lambda_\parallel = 7150 \pm 150$ Å, or equivalently that $\lambda_1 = \lambda_\parallel$ and that $\lambda_3 = 4220 \pm 90$ Å. Using $\lambda_{ave}^3 = \lambda_1^2 \lambda_3 = \lambda_\perp^2 \lambda_\parallel$ we get $\lambda_{ave} = 6000 \pm 75$ Å. For comparison, on unannealed crystals otherwise prepared in the same way, μ^+SR measurements give $\lambda_1 = 8200$ Å and $\lambda_3 = 7100$ Å at 50 mK.

There are several features of the data which cannot be explained in the context of the AL theory. First, the vortex lattice is orientationally registered with the crystal lattice, whereas all orientations are equally favorable. We expect that only the two orientations which are consistent with the symmetry of the crystal are allowed, since these would be stabilized by crystalline anisotropy terms. Second, while in the AL theory $H_{10} = H_{01}$, we find that

$H_{10}/H_{01} = 1.35 \pm 0.20$ for $H = 4.25$ kG. Third, in the AL theory there is no natural explanation for the gradual change in lattice distortion we observe with increasing field. These can be satisfactorily explained [30,31], at least qualitatively, by considering the effects of higher-order Fermi-surface and gap anisotropy when nonlocal electrodynamics is relevant (in this case when $H > H_c \sim 500$ G). The nonlocal terms, which can be considered perturbatively, provide an extra source of anisotropy beyond the more trivial AL anisotropy, breaking the degeneracies mentioned above and allowing for a modest field dependence of the lattice distortion.

In conclusion, our measurements on UPt_3 show a conventional vortex lattice in a moderately anisotropic system. We observe significant effects of anisotropy, which do not prove, but are nevertheless consistent with, substantial gap anisotropy. We find no evidence at either low or high fields for a vortex lattice which is unconventional in either its structure or its composite vortices. Nor do we find evidence of a change in the vortex lattice at $H \sim 6$ kG which could account for the observed signature in torsional oscillator and ultrasound measurements. However, this does not preclude more subtle effects beyond our sensitivity, or in other configurations of field, temperature, and orientation. It is also conceivable that the vortex lattice or the measuring probe itself (i.e., sound waves) is coupling to another subsystem such as the domain walls in the antiferromagnetic state which is known to change near the locus of the anomalies [32].

We gratefully acknowledge technical assistance from T. T. M. Palstra, A. P. Ramirez, and the Risø technical staff, as well as valuable discussions with J. Als-Nielsen, E. M. Forgan, P. L. Gammel, J. Kjems, V. G. Kogan, and A. Sudbø. This program was made possible by generous grants from the Danish Natural Science Foundation.

---

[a]Also at Cornell University, Ithaca, NY 14853.
[b]Now at Johns Hopkins University, Baltimore, MD 21218.
[c]Also at University of Konstanz, Konstanz 7750, Federal Republic of Germany.
[d]Now at Eidgenössische Technische Hochschule Zürich-Hönggerberg, Zurich, Switzerland.
[e]c/o G. Lonzarich, Cavendish Laboratory, Cambridge, United Kingdom.

[1] M. Sigrist and K. Ueda, Rev. Mod. Phys. **63**, 239 (1991); R. N. Kleiman, "Experimental Evidence for Higher-l Pairing in Heavy Fermion Superconductors" (to be published); D. J. Bishop *et al.*, Phys. Rev. Lett. **53**, 1009 (1984).
[2] B. S. Shivaram *et al.*, Phys. Rev. Lett. **56**, 1078 (1986).
[3] C. Broholm *et al.*, Phys. Rev. Lett. **65**, 2062 (1990); in this paper $\lambda_\perp$ and $\lambda_\parallel$ denote the principal values of the penetration depth tensor.
[4] G. E. Volovik and L. P. Gor'kov, Pis'ma Zh. Eksp. Teor. Fiz. **39**, 550 (1984) [JETP Lett. **39**, 674 (1984)].
[5] R. N. Kleiman *et al.*, Phys. Rev. Lett. **62**, 328 (1989).
[6] Y. J. Qian *et al.*, Solid State Commun. **63**, 599 (1987); V. Muller *et al.*, Phys. Rev. Lett. **58**, 1224 (1987).
[7] R. A. Fisher *et al.*, Phys. Rev. Lett. **62**, 1311 (1989).
[8] A. Schenstrom *et al.*, Phys. Rev. Lett. **62**, 332 (1989).
[9] G. E. Volovik, J. Phys. C **21**, L215 (1988); **21**, L221 (1988); R. Joynt, Supercond. Sci. Technol. **1**, 210 (1988); T. A. Tokuyasu *et al.*, Phys. Rev. B **41**, 8891 (1990); R. Joynt, Europhys. Lett. **16**, 289 (1991).
[10] A. P. Ramirez (unpublished).
[11] P. G. de Gennes and J. Matricon, Rev. Mod. Phys. **36**, 45 (1964).
[12] D. Cribier *et al.*, Phys. Lett. **9**, 106 (1964).
[13] For a summary see J. Schelten, in *Anisotropy Effects in Type II Superconductors*, edited by H. W. Weber (Plenum, New York, 1977), p. 113.
[14] D. K. Christen *et al.*, Phys. Rev. B **21**, 102 (1980).
[15] J. Schelten *et al.*, J. Low Temp. Phys. **14**, 213 (1974).
[16] E. M. Forgan *et al.*, Nature (London) **343**, 735 (1990).
[17] V. G. Kogan, Phys. Lett. **85A**, 299 (1981).
[18] K. Takanaka and H. Ebisawa, Prog. Theor. Phys. **47**, 1781 (1972); L. Dobrosavljevic and H. Raffy, Phys. Status Solidi (b) **64**, 229 (1974); K. Takanaka, Phys. Status Solidi (b) **68**, 623 (1975).
[19] L. J. Campbell *et al.*, Phys. Rev. B **38**, 2439 (1988).
[20] Takanaka's type (a) lattice [30] is equivalent to Campbell's (B)1 lattice [19]. This lattice type is observed in technetium (Tc) with $\alpha = 52.5°$ corresponding to $m_1/m_3 = 1.77$. Takanaka's type (b) lattice is equivalent to Campbell's (B)3 lattice which is observed in UPt_3. Takanaka's statement that "only one kind of flux line lattice [type (a)] is observed in experiment" refers only to the Tc experiment with $\mathbf{H} \perp \hat{\mathbf{c}}$. For tilted field (intermediate between $\mathbf{H} \perp \hat{\mathbf{c}}$ and $\mathbf{H} \| \hat{\mathbf{c}}$) the (B)1 lattice is the more favorable [19]. Neither of the above experiments directly bears on that result because for $\mathbf{H} \perp \hat{\mathbf{c}}$ both lattice types have equal energies.
[21] A. de Visser *et al.*, J. Magn. Magn. Mater. **43**, 43 (1984).
[22] T. Oguchi and A. Freeman, J. Magn. Magn. Mater. **52**, 174 (1985); R. C. Albers *et al.*, Phys. Rev. B **33**, 8116 (1986); C. S. Wang *et al.*, J. Phys. F **16**, L287 (1986).
[23] L. Taillefer *et al.*, J. Magn. Magn. Mater. **63&64**, 372 (1987); L. Taillefer *et al.*, Phys. Rev. Lett. **60**, 1570 (1988).
[24] G. Bruls *et al.*, Phys. Rev. Lett. **65**, 2294 (1990).
[25] S. Adenwalla *et al.*, Phys. Rev. Lett. **65**, 2298 (1990).
[26] We define $H'_{c2}(1) = dH_{c2}/dT(T/T_c = 1)$. The discrepancy between $H_{c2}(0)$ values and $H'_{c2}(1)$ values is apparent because the $H_{c2}(T)$ curves for $\mathbf{H} \perp \hat{\mathbf{c}}$ and $\mathbf{H} \| \hat{\mathbf{c}}$ cross at $T/T_c \approx 0.4$. We have chosen the lower-T_c branches for $H'_{c2}(1)$ and the higher-H branches for $H_{c2}(0)$.
[27] L. P. Gor'kov and T. K. Melik-Borkhudurov, Zh. Eksp. Teor. Fiz. **45**, 1493 (1963) [Sov. Phys. JETP **18**, 1031 (1964)].
[28] E. H. Brandt, Phys. Status Solidi (b) **51**, 345 (1972).
[29] M. P. Kemoklidze, Zh. Eksp. Teor. Fiz. **47**, 2247 (1964) [Sov. Phys. JETP **20**, 1505 (1964)]; J. Schelten *et al.*, Phys. Status Solidi (b) **48**, 619 (1971).
[30] K. Takanaka, in *Anisotropy Effects in Type II Superconductors* (Ref. [13]), p. 93.
[31] K. Fischer and H. Teichler, Phys. Lett. **58A**, 402 (1976).
[32] G. Aeppli *et al.*, Phys. Rev. Lett. **63**, 676 (1989).

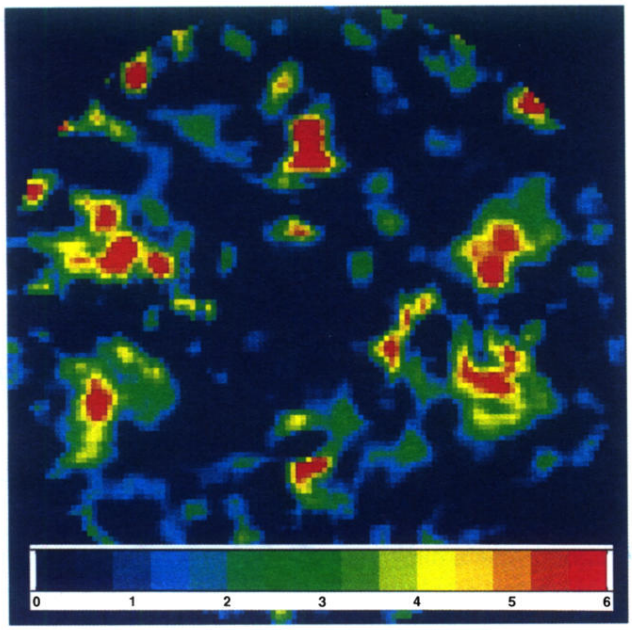

FIG. 1. The 2D intensity profile of the $(\hat{\mathbf{a}}^*,\hat{\mathbf{c}}^*)$ plane of the vortex lattice in UPt_3. The $\hat{\mathbf{c}}^*$ axis is vertical, and the $\hat{\mathbf{a}}^*$ axis is horizontal. The region shown (± 0.0159 Å^{-1}, ± 0.0158 Å^{-1}) corresponds to 60×60 pixels. The intensities are in units of counts/h pixel. The data were taken at $H=4.25$ kG, $T=50$ mK, with $\lambda_n=9.78$ Å and $\Delta\lambda/\lambda=0.36$, using $H=4.25$ kG, $T=600$ mK as a background and represent a total counting time of ≈ 33 h. The integrated intensity of one of the Bragg peaks corresponds to ≈ 250 counts/h. The statistical errors in the peak intensities are $\approx 10\%$. The background scattering is discussed quantitatively in the text.